environmental microbiology

Environmental Microbiology (2019) **21**(7), 2273–2289 doi:10.1111/1462-2920.14605

Differential gene expression associated with fungal trophic shifts along the senescence gradient of the moss *Dicranum scoparium*

Ko-Hsuan Chen,[1*] **Hui-Ling Liao**,[2] **Jean-Philippe Bellenger**[3] **and François Lutzoni**[1]

[1]*Department of Biology, Duke University, Durham, NC, USA.*

[2] *North Florida Research and Education Center, University of Florida, Quincy, FL, USA.*

[3]*Department of Chemistry, University of Sherbrooke, Sherbrooke, QC, Canada.*

Summary

Bryophytes harbour microbiomes, including diverse communities of fungi. The molecular mechanisms by which perennial mosses interact with these fungal partners along their senescence gradients are unknown, yet this is an ideal system to study variation in gene expression associated with trophic state transitions. We investigated differentially expressed genes of fungal communities and their host *Dicranum scoparium* across its naturally occurring senescence gradient using a metatranscriptomic approach. Higher activity of fungal nutrient-related (carbon, nitrogen, phosphorus and sulfur) transporters and Carbohydrate-Active enZyme (*CAZy*) genes was detected toward the bottom, partially decomposed, layer of the moss. The most prominent variation in the expression levels of fungal nutrient transporters was from inorganic nitrogen-related transporters, whereas the breakdown of organonitrogens was detected as the most enriched gene ontology term for the host *D. scoparium*, for those transcripts having higher expression in the partially decomposed layer. The abundance of bacterial rRNA transcripts suggested that more living members of *Cyanobacteria* are associated with the photosynthetic layer of *D. scoparium*, while members of *Rhizobiales* are detected throughout the gametophytes. Plant genes for specific fungal–plant communication, including defense responses, were differentially expressed, suggesting that different genetic pathways are involved in plant-microbe crosstalk in photosynthetic tissues compared to partially decomposed tissues.

Received 20 November, 2018; revised 19 March, 2019; accepted 21 March, 2019. *For correspondence. E-mail kc178@duke.edu; Tel. 850-875-7197; Fax 352-846-6617.

Introduction

Plant–fungal symbiotic associations are common across different lineages of land plants. These symbioses include pathogenic, mycorrhizal and endophytic interactions (van der Heijden *et al.*, 2015; Peay *et al.*, 2016; Lutzoni *et al.*, 2018). Mosses (phylum Bryophyta) are a major component of boreal, alpine and arctic vegetations, and contribute significantly to global nutrient cycles (Brown and Bates, 1990; Turetsky, 2003; Lenton *et al.*, 2016). Generally, mosses are observed to lack fungal symbionts such as mycorrhizal fungi (Field *et al.*, 2015), but studies during the last decade have consistently reported that they host rich fungal communities (Davey and Currah, 2006, 2007; Stenroos *et al.*, 2010; U'Ren *et al.*, 2010, 2012). Despite the uncertainty about the phylogenetic relationships among bryophytes and their affiliations to tracheophytes (Puttick *et al.*, 2018), fungal interactions with early diverging land plants could unveil ancestral genetic mechanisms associated with the origin of fungal endophytism (Delaux *et al.*, 2013; Ponce de León and Montesano, 2017; Lutzoni *et al.*, 2018). Perennial mosses can have a natural senescence gradient that is ideal to study the functions of fungal endophytes and their life cycles. Recent advancements in next-generation sequencing opened the possibility to decipher moss–fungus interactions through the study of metatranscriptomes from mosses in their natural habitats.

Nutrient exchanges play key roles in plant–fungal interactions. For mycorrhizae, plants serve as a carbon source for the interacting fungi, whereas fungi provide nitrogen and phosphorus to the plants (Bonfante and Genre, 2010). Many nutrient transporters have been identified in these interactions, such as ammonium, urea, nitrate, amino acid, phosphate and hexose transporters (Bonfante and Genre, 2010; Martin *et al.*, 2010; Almario *et al.*, 2017). Mycorrhizal fungi also enhance the sulfur uptake of plants (Gahan and Schmalenberger, 2014). Similar nutritional interactions have been reported for fungal endophytes and non-mycorrhizal fungi associated with plant roots. Studies on above-ground

plant–fungal symbioses mainly focused on pathogenic interactions. Such studies reported various fungal transporters, including sugar and amino acid transporters, that are upregulated during fungal infections (O'Connell *et al.*, 2012). However, trophic states of fungi can be dynamic. Some endophytic fungi can colonize also dead tissues of their host plant species (Osono and Hirose, 2011; Chen *et al.*, 2018). This substrate shift might be expected to affect the activity of these transporters. Fungal carbohydrate-active enzymes (CAZys) play critical roles in the decomposition of plant materials (Eastwood *et al.*, 2011; Zhao *et al.*, 2013; Riley *et al.*, 2014; Hesse *et al.*, 2015). The genes encoding CAZys are largely found in saprotrophic fungi but are also present in many mycorrhizal-forming fungi, plant pathogenic fungi and endophytic fungi (Ohm *et al.*, 2012; Kohler *et al.*, 2015; Wang *et al.*, 2015; Martino *et al.*, 2018). Expression patterns of fungal *CAZy* genes when interacting with plant tissues at different levels of senescence can provide insights into the trophic states of fungi inhabiting these tissues and their capacity to switch between endophytism and saprotrophism. Besides nutrient exchange, plant and fungal interactions involve specific molecular crosstalk (Zuccaro *et al.*, 2011; Plett *et al.*, 2014; Liao *et al.*, 2016; Almario *et al.*, 2017). For example, interactions between microbial effectors (often small secreted proteins) and plant receptors (e.g., nucleotide-binding leucine-rich repeats [NB-LRR]) that are part of the plant defensive response can lead to virulence in pathogen–plant interactions or compatible mutualistic associations (Plett *et al.*, 2014; Lo Presti *et al.*, 2015; Liao *et al.*, 2016).

Plant-associated fungal communities are shaped by factors including plant host species, plant compartments (e.g., leaf versus root), biogeographical areas (Rodriguez *et al.*, 2009; U'Ren *et al.*, 2010, 2012; Bonito *et al.*, 2014; Chang *et al.*, 2016) and other environmental factors such as temperature, precipitation and pH (Rudgers *et al.*, 2014; Glassman *et al.*, 2017; Barnes *et al.*, 2018). However, changes in fungal communities do not always result in changes of their functions. A study focusing on soil fungal communities and extracellular enzyme activities revealed that despite endemism of fungal community composition at various sampling sites, high functional convergences were detected (Talbot *et al.*, 2014). On the other hand, another study reported that functional differences were associated with shifts in fungal communities (Walker *et al.*, 2014). Functional transitions have not been investigated for fungal communities colonizing a physically connected and continuous senescence gradient. This is because plant organs at different stages of senescence are usually separated in time and space. The latter adds confounding effects that limit the conclusiveness of studies conducted on the great majority of land plants. Trophic state switches between biotrophic and saprotrophic life styles have been demonstrated in a few root-associated endophytic fungi (Zuccaro *et al.*, 2011; Zhou *et al.*, 2018). However, studies focusing on life style transitions are still lacking for fungal endophytes inhabiting above-ground plant tissues.

The perennial moss *Dicranum scoparium* has a continuous senescence gradient that includes top (photosynthetic), middle (senescent) and bottom (decomposing) layers along its acrocarpous gametophyte (Fig. 1). It is known to harbour a high diversity of fungi (U'Ren *et al.*, 2010; Davey *et al.*, 2017; Chen *et al.*, 2018). These features make *D. scoparium* an ideal system to study the capacity of fungi to switch function or for a mycelium to have multiple functions simultaneously. Our previous study (Chen *et al.*, 2018) revealed that fungal communities were structured according to the senescence gradient of *D. scoparium.* We also found that some fungi were active (based on their nuclear ribosomal RNA [nrRNA] gene expression levels) (Chen *et al.*, 2018) throughout the three layers of the gametophytes. Here, we investigated the functions of these fungal communities and of the moss host *D. scoparium* across the same senescence gradient using messenger RNA (mRNA). We hypothesized that 1) the activity of crucial nutrient transporters and CAZys of these fungi changes in response to the degree of plant senescence; 2) certain nutrient transporters have higher expression levels in different senescence layers, reflecting their different ecological roles; 3) functional taxonomic groups of fungal nutrient transporters agree with the changes in fungal communities we detected using fungal nrRNA; and 4) plant functions change along its senescence gradient, and the changes not only reflect its physiological state but also the different fungal groups it is interacting with in each layer. To test these hypotheses, we investigated the metatranscriptomes of *D. scoparium* in each of these three main layers from specimens collected in their natural habitats, and searched for functional genes that are likely related to fungal–plant nutrient exchanges: carbon, nitrogen (subdivided into organic nitrogen [amino acids] and inorganic nitrogen), phosphorus and sulfur. We prepared a transcriptome reference data set from an axenic *D. scoparium* culture to enable us to extract molecular data belonging to the moss from the complex environmental metatranscriptomes. Because of their integral importance in plant–fungal symbiotic systems, we also investigated bacterial communities based on their nrRNA for a more comprehensive understanding of holobiont interactions.

Results

Taxonomic transcripts binning of environmental D. scoparium *metatranscriptomes*

A wide range of microorganisms and a complex metatranscriptome were revealed through the binning process of 2,243,417 assembled transcripts from environmental samples of *D. scoparium.* The percentage of reads mapping to plants (mean mapping percentage: top layer 57.6% $\pm$ 5.5%, middle

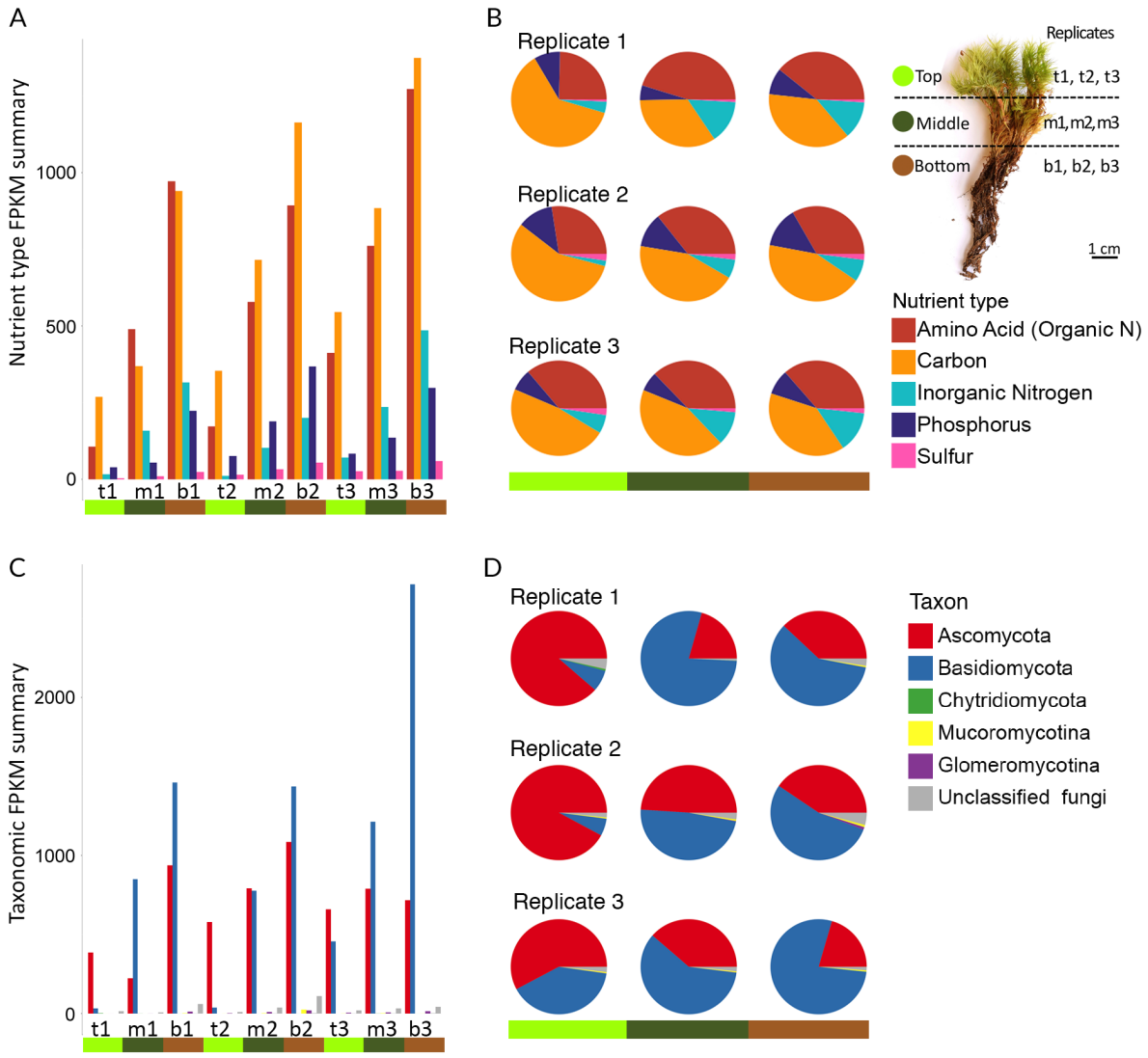

Fig. 1. Fungal nutrient transporter gene expression from metatranscriptomic data across three layers (top, middle, bottom [t, m, b]) of the senescence gradient of *Dicranum scoparium* for three replicates (t1, m1, b1; t2, m2, b2; t3, m3, b3).
A. Nutrient-type Fragments Per Kilobase of transcript per Million mapped reads (FPKM) sums.
B. Nutrient-type FPKM ratios.
C. Taxon FPKM sums based on nutrient transporter gene expression levels.
D. Taxon FPKM ratios based on nutrient transporter gene expression levels.

layer 46.2% ± 11.8%, bottom layer 22.9% ± 6.5%) was always the highest compared to the percentage of reads mapped to other taxonomic categories, except from the bottom layer of the third replicate (b3 in Supporting Information Fig. S2). The percentage of reads that mapped to fungi showed a consistent increase toward the bottom layer (mean mapping percentage: top layer 8.9% ± 1.0%, middle layer 11.9% ± 2.3%, bottom layer 16.1% ± 5.2%) of the gametophytes, that is, across the three replicates, contrary to *D. scoparium* read percentages that decreased from the top to the bottom layer. Overall, the binning process revealed a high diversity of organisms putatively associated with *D. scoparium*, but as expected the host plant itself is the main active organism. The expression of fungal nutrient transporter and *CAZy* genes in the top layer demonstrated the least degree of variation among replicates compared to the middle and bottom layers (Supporting Information Fig. S3A and B), whereas the contrary was observed for the overall gene expression of plants, where the greatest inter-replicate variation in gene expression was observed in the top layer compared to the other two layers (Supporting Information Fig. S3C).

Functional transition of fungal nutrient transporters along a senescence gradient

Our workflow detected 3112 fungal nutrient transporter genes (amino acids [organic nitrogen] = 1247, carbon = 1230,

Table 1. Numbers of significantly differentially expressed genes based on the Fungal Nutrient Transporter Database (FNTD) and the Axenic *Dicranum scoparium* Transcriptome Database (ADTD) references (FDR < 0.05).

	Top upregulated	Middle upregulated	Bottom upregulated
Ref.: FNTD			
Top versus bottom	19	NA	155
Middle versus bottom	NA	0	2
Top versus middle	1	5	NA
Ref.: ADTD			
Top versus bottom	1724	NA	545
Middle versus bottom	NA	314	182
Top versus middle	1202	261	NA

inorganic nitrogen = 161, phosphorus = 350 and sulfur = 124; for annotations, see Supporting Information Tables S3–S7). Overall bigger differences were observed among top versus bottom layers compared to top versus middle or middle versus bottom layers. The middle layer expression levels were often intermediary, and therefore, were often not significantly distinguishable from the top or bottom layers (Supporting Information Fig. S3A; Table 1). These transporters are distributed across the fungal tree of life (Ascomycota, Basidiomycota, Chytridiomycota, Mucoromycotina, Glomeromycotina and unclassified taxa, i.e., assigned to fungal taxa with uncertain taxonomic placements) (Supporting Information Fig. S4). All five categories of fungal nutrient transporters are more highly expressed toward the bottom layer (Fig. 1A). Besides this overall trend, the most significant proportional increase was detected for inorganic nitrogen transporter genes (Fig. 1B, Welch's two-sample *t* test between the top and bottom layers: *t* statistics = −3.13, P value = 0.04). Although amino acid (organic nitrogen) transporters proportionally increased toward the bottom layer, this trend is not significant (Fig. 1B; Supporting Information Table S8, Welch's two-sample *t* test between the top and bottom layers: *t* statistics = −1.73, P value = 0.18). Based on a Differential Gene Expression (DGE) test, all individual inorganic nitrogen-related and sulfate-related transporter genes detected to be significantly differentially expressed (FDR < 0.05, absolute $\log_2$ fold change > 2) had higher expressions in the bottom layer. The same was true for most of the significantly differentially expressed carbon-, amino-acid- and phosphorus-related transporter genes; however, some had higher expression in the top layer of the moss (Fig. 2A).

Of the 161 inorganic nitrogen transporter genes detected in this study, only five were nitrate/nitrite transporters, the rest being ammonium transporters. Contrary to ammonium transporter genes and most nutrient genes, all nitrate/nitrite transporters (*CrnA*/*NrtA*) were more expressed (although not significantly, FDR > 0.05) in the top layer of *D. scoparium* (Fig. 2B). The phylogenetic analysis of ammonium transporters revealed that all ammonium transporters detected here belong to the clade MEPγ (Supporting Information Fig. S5).

Taxonomic transition of fungal nutrient transporters along a senescence gradient

The sums of Fragments Per Kilobase of transcript per Million mapped reads (FPKM) showed that fungal activity of the two dominant phyla (Ascomycota and Basidiomycota) increased toward the bottom layer of the gametophytes, especially for Basidiomycota (Fig. 1C). When the proportional activities were examined, Ascomycota contributed the most compared to other phyla/subphyla in the top layer but its relative activity decreased in the middle and bottom layers (Fig. 1D; Supporting Information Table S9). Nearly all 19 upregulated nutrient transporter genes with significantly higher expression levels in the top layer belonged to Ascomycota (with the exception of three genes from Basidiomycota; Fig. 2A). The genes that were significantly more expressed in the bottom layer belong to several phyla and subphyla, including Ascomycota, Basidiomycota, Mucoromycotina, Glomeromycotina and Chytridiomycota (Fig. 2A).

Fungal CAZy *activity along the senescence gradient*

A total of 2447 fungal *CAZy* genes (Supporting Information Table S10) were identified. The overall fungal *CAZy* gene expression increases toward the bottom layer of the gametophytes (Fig. 3A). The taxonomic compositions of the active *CAZy* genes change across the layers, showing Basidiomycota being proportionally more active in the bottom layer of the gametophytes (Fig. 3B; Supporting Information Table S11). Of the top 30 expressed *CAZy* genes across the gametophytes, all of them were more active in the bottom or middle layer (Fig. 3). Nearly all top 30 *CAZy* genes are found in genomes of Basidiomycota (except for four in Ascomycota).

Diverse active bacterial communities across D. scoparium *senescence gradient*

Many nitrogen fixers were detected in *D. scoparium* samples (Fig. 4; Supporting Information Table S12). The percentages of reads belonging to the phylum *Cyanobacteria* (*Nostocales*, *Oscillatoriales* and *Synechococcales*) are higher in the top layer (Fig. 4) (31.4% ± 14.7%) compared to the bottom layer (1.4% ± 1.3%) (ANOVA test: *F* statistics = 10.8, P value = 0.01; Tukey's HSD: top versus bottom P value = 0.01). The heterocystous cyanobacteria *Cylindrospermum* and *Nostoc* were the main contributors to this trend (Supporting Information Table S12). Reads from members of the *Rhizobiales* are consistent across the senescence gradient of *D. scoparium*

Fig. 2. Expression levels of fungal nutrient-related transporters differentially expressed between the top and bottom layer of the moss *Dicranum scoparium.*
A. Amino acid (organic nitrogen), carbon, inorganic nitrogen, phosphorus and sulfur transporters (FDR < 0.05, Log2 fold change > 2).
B. Nitrate/nitrite transporters.

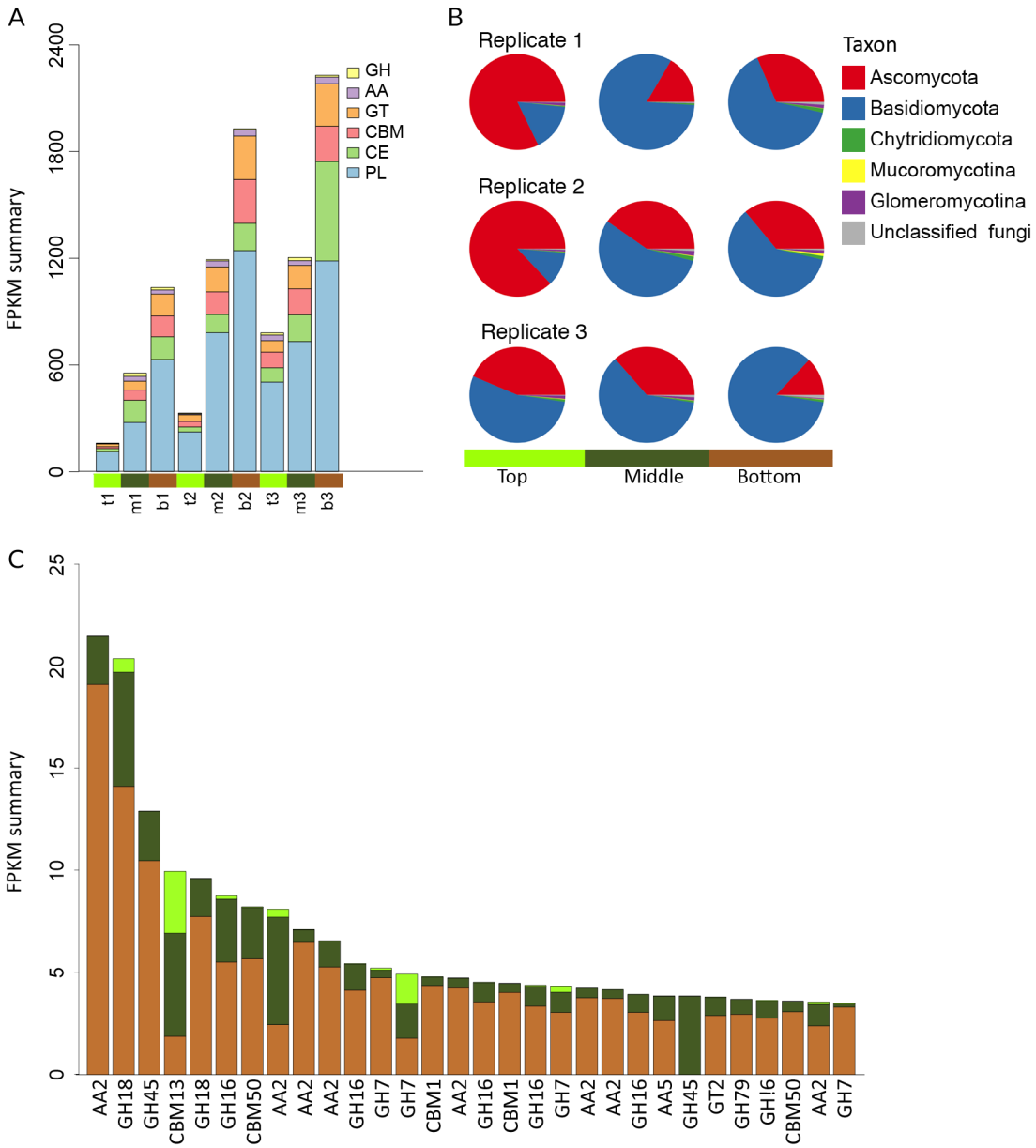

Fig. 3. Expression levels and taxonomic affiliations of fungal Carbohydrate-Active enZymes (CAZy).
A. Categories of fungal CAZy Fragments Per Kilobase of transcript per Million mapped reads (FPKM) sums across layers and replicates of the moss *Dicranum scoparium*.
B. Taxonomic affinities of fungal CAZy FPKM ratios across layers and replicates.
C. Top 30 ranked *CAZy* genes of fungi associated with *Dicranum scoparium*. The *y*-axes correspond to the mean ratios of reads mapped to the individual *CAZy* gene of the three replicates. Colours in the bars of this histogram refer to specific layer fractions as shown in panel B, that is, pale green, top; dark green, middle; and brown, bottom layer. AA, auxiliary activities; CBM, carbohydrate-binding module; CE, carbohydrate esterases; GH, glycoside hydrolases; GT, glycosyl transferases; PL, polysaccharide lyases.

(ANOVA test: *F* statistics = 3.02, P value = 0.12, Tukey's HSD: top versus bottom P value = 0.21).

Differentially expressed moss genes along a senescence gradient

We examined the differentially expressed genes of *D. scoparium* across its senescence gradient to confirm that our sampling scheme captured the different physiological states of this plant. Overall, the expression level of the host plant in the middle layer was more similar to the bottom layer (Supporting Information Fig. S3C; Table 1). We detected 2269 significantly differentially expressed moss genes between the top and bottom layers (Table 1). When we searched for defense/symbiosis-related genes that are likely to be relevant to inter-species interactions, we recovered

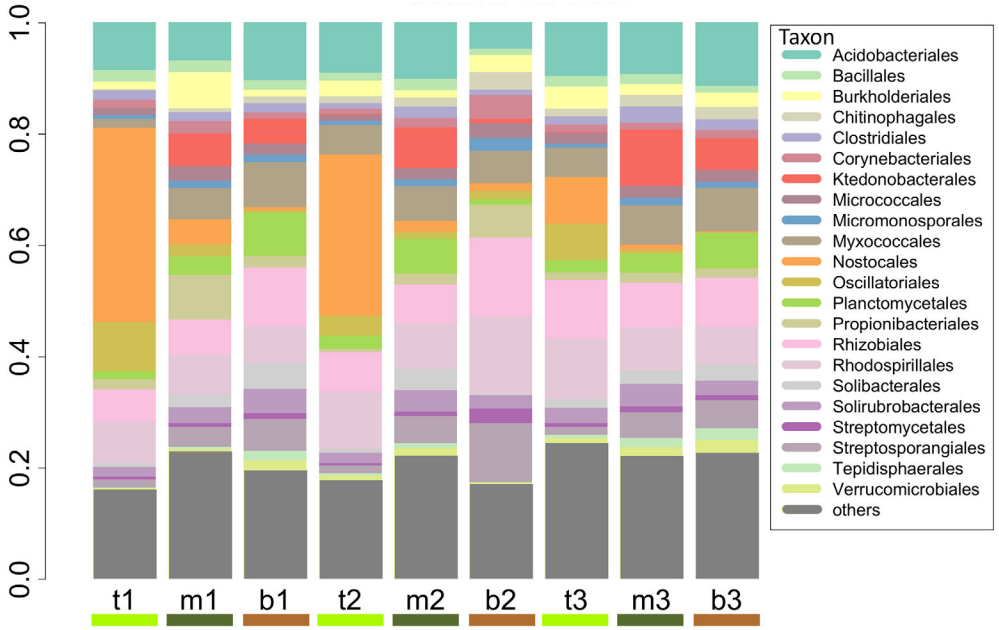

Fig. 4. Bacterial communities at the order level across the senescence gradient of *Dicranum scoparium* for three replicates. The ratios were calculated based on reads mapped to the *16S* gene of individual metatranscriptome.

many microbe–plant recognition (leucine-rich repeat receptors, lectin receptors, chitin elicitor receptors) and defense response genes (aldehyde oxidases, monooxygenases, lipoxygenases) (Fig. 5) (FDR < 0.01, Supporting Information Tables S13 and S14). However, some common transcripts (i.e., DESeq2 expression base mean > 500, log2 fold change < 2, FDR > 0.05) related to LRR/defense/symbiosis were consistently transcribed across layers, suggesting that a similar baseline interaction might be maintained throughout the gametophytes (Supporting Information Fig. S6). Genes with higher transcription levels (P value < 0.01) in the top layer were mostly related to intra-species functions such as growth and primary metabolism, such as photosynthesis, chloroplast, transport, membrane and cell wall development (Supporting Information Table S15). Fewer genes with GO terms were enriched for the bottom layer, but many were related to catabolic processes (Supporting Information Fig. S7 and Table S16). The most enriched moss GO term in the bottom layer is associated with "organonitrogen compound catabolic process".

Discussion

Fungal nutrient-related transporters across the senescence gradient of D. scoparium

The overall higher abundance of fungal nutrient-related transporters (Fig. 1 and Table 1) is characterized by higher fungal activities toward the bottom layer of *D. scoparium* (Chen *et al.*, 2018) and higher fungal biomass in the bottom layer of this moss (Davey *et al.*, 2012, 2013). Most of the transporters significantly upregulated in the top layer were from fungi in the classes Leotiomycetes and Eurotiomycetes, which is in agreement with our previous finding that these two fungal classes have high activities (using nrRNA transcripts as a proxy) in the top layer of *D. scoparium* (Chen *et al.*, 2018).

The myo-inositol transporter is among the few fungal nutrient transporters that were only significantly expressed (FDR < 0.05, absolute $\log_2$ fold change > 2) in the photosynthetic layer of *D. scoparium* (Fig. 2). The acquisition of myo-inositol has been shown to be relevant to ectomycorrhizal mutualism (Ceccaroli *et al.*, 2010). Also, inositol has been shown to be related to virulence in certain animal pathogenic fungi such as *Cryptococcus* (Xue, 2012) but not in *Candida* (Chen *et al.*, 2008). These previous studies suggested that inositol has diverse functions in different fungi and that its role in moss–fungus interactions is not well understood. We detected multiple lactose permeases representing an array of fungal taxa including Pezizomycetes and Orbiliomycetes (Fig. 2). Previous studies detected higher expression of lactose permease in tuber–ectomycorrhizal (ECM) roots (Ceccaroli *et al.*, 2010) compared to free living mycelia. Our previous work identified several ECM fungi (e.g., *Russula* and *Lactarius*) associated with the bottom layer of *D. scoparium* (Chen *et al.*, 2018). Carleton and Read (1991) reported nutrient transfers from mosses to trees through ECM fungi. Perhaps a similar interaction of ECM–moss rhizoids with ECM–tree roots is involved here.

Genes of phosphate transporters detected to be significantly more expressed (FDR < 0.05, absolute $\log_2$ fold change >2) in the bottom layer, compared to the top layer,

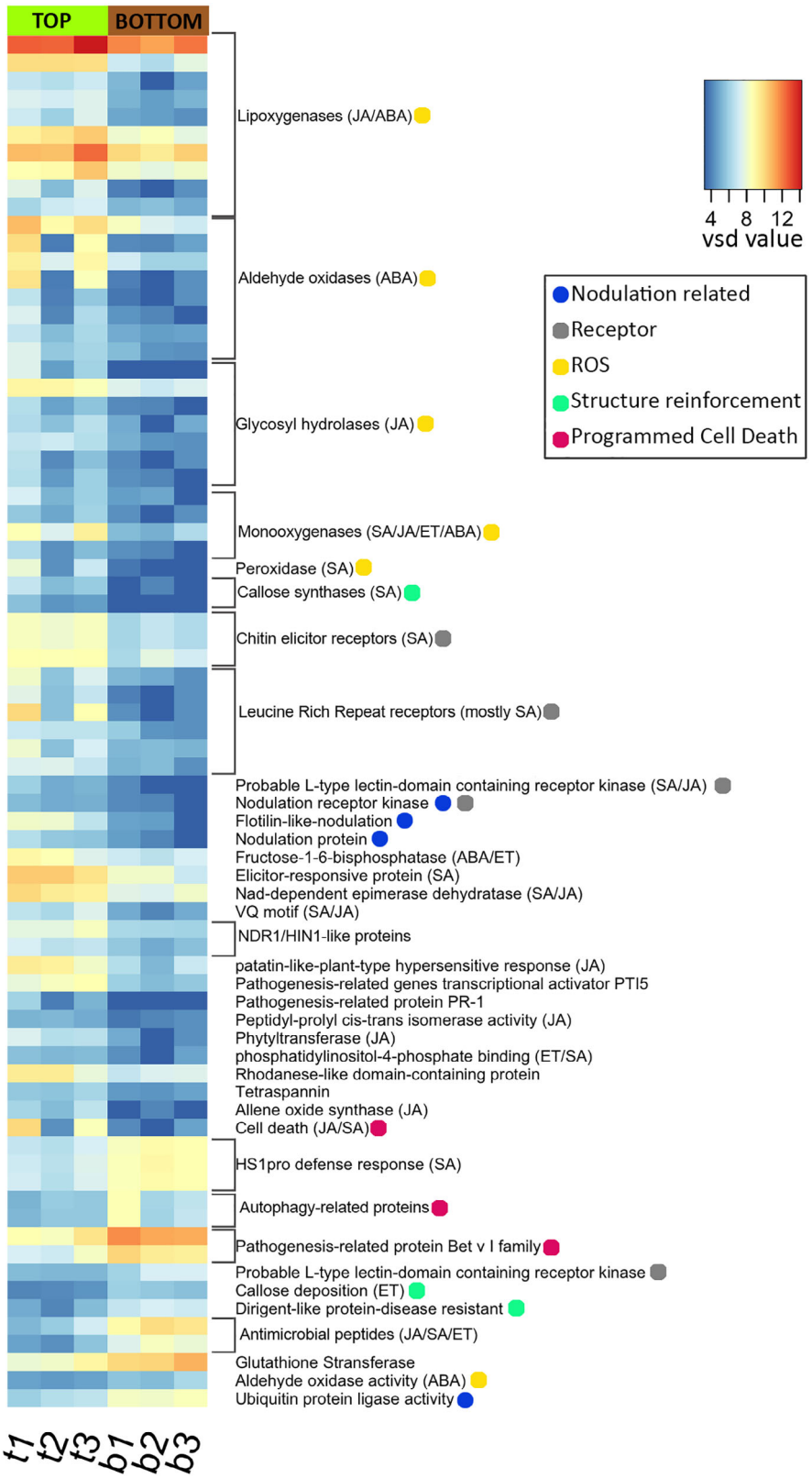

Fig. 5. *Dicranum scoparium* defense/symbiosis-related genes detected as highly differentially expressed when comparing top and bottom layers (FDR < 0.01). ROS, reactive oxygen species; SA, salicylic acid; ABA, abscisic acid; JA, jasmonic acid; ET, ethylene.

belong to multiple phyla/subphyla (Fig. 2) and shared high sequence and domain structure similarity with known phosphate transporters (*Pho88*, *Pho84*, *Pho5*) involved in root–mycorrhiza (Xie *et al.*, 2016) and root–endophyte (Almario *et al.*, 2017) phosphate translocation. We cannot rule out the possibility that the phosphates transported by these

fungi are for their own usage instead of being for the plant host. Surprisingly, three fungal phosphate transporters were more expressed in the top layer of this moss (Fig. 2). The 3D protein structure analysis (Yang *et al.*, 2015) confirmed that these three proteins also have the ability to transport glucose and maltose, which are substrates more likely to be taken up by biotrophic fungi in the upper layer of a moss. Future research to understand phosphate transfer in moss–fungal associations will be critical to better understand bryophyte–fungal symbioses and above-ground fungal endophytism in general.

Sulfate transporters produced by Basidiomycota fungi were significantly more expressed in the bottom layer (FDR < 0.05, absolute $\log_2$ fold change > 2), suggesting their roles in mobilizing inorganic sulfur (Gahan and Schmalenberger, 2014). Most sulfur in plants occurs in the form of sulfur-containing amino acids, whereas soils are more rich in inorganic sulfur (sulfates mostly) (Giovanelli, 1987; Linder, 2012). The bottom layer of acrocarpous mosses has a much closer connection to the soil, and the mycelium (particularly of basidiomycetes) likely spans both soil and plant material, meaning that the differential expression of these transporters may be a reflection of the sulfur source available to the fungus.

Amino acids can be an organic source for mainly nitrogen and also for sulfur and carbon. Biotrophic fungi interacting with living plants can uptake amino acids from their host plant (Hall and Williams, 2000; Struck, 2015). Two fungal proline transporter genes were detected to have significantly higher expression in the top layer, while the other eight were expressed more in the bottom layer (FDR < 0.05, absolute $\log_2$ fold change > 2) (Fig. 2). Proline content increases when plants are stressed (Verslues and Sharma, 2010) and during the natural dehydration/hydration cycle of mosses (Liu *et al.*, 2016). It might be readily available for fungal members of Ascomycota (mostly Leotiomycetes/Eurotiomycetes) and also in the bottom layer by members of Basidiomycota (mostly Agaricomycetes) (Fig. 2). Several sulphur-containing amino acid transporters (cysteine, methionine and glutathione) (Fig. 2) were also detected to be significantly more expressed (FDR < 0.05, absolute $\log_2$ fold change > 2) in the bottom layer (Giovanelli, 1987). The direction of the translocation of these amino acids (from fungi to plants or vice versa) remains to be determined.

Ammonium versus nitrate transport by fungi

An increase in fungal inorganic nitrogen-related transporter activity was detected toward the bottom layer of *D. scoparium* (Fig. 1), which is in accordance with the degree of decomposition of moss tissues. Our observation that all fungal nitrate transporters were more active in the photosynthetic top layer compared to most of the ammonium transporters, which were more highly expressed in the bottom layer (Fig. 2), suggest a different nitrogen source utilization strategy by moss-associated fungi. The main sources of inorganic nitrogen for fungi in the bottom layer are from soil, including the decomposing litter, whereas atmospheric deposition is likely the main source of nitrogen for fungi in the top layer of mosses. Sparks *et al.* (2007) and the public atmospheric monitoring database (Ambient Air Concentrations, CASTNET, United States Environmental Protection Agency, 2012) reported that the nitrogen deposition in Duke Forest is a mixture of nitrate and ammonium. Therefore, both are available to fungi in the top layer of mosses. Ammonium, as opposed to nitrate, has been shown to be the preferred inorganic nitrogen source for most fungi (Finlay *et al.*, 1992; Keller, 1996; Zhou *et al.*, 2002) and for several moss species (Liu *et al.*, 2013). Therefore, potential competition for ammonium between the moss and fungi may occur in the photosynthetic portions of the moss. Under such competition, nitrate may become the most accessible inorganic nitrogen source for fungi, resulting in the higher observed expression of fungal nitrate in the top layer of the moss. Low nitrification rates beneath moss mats have been observed (Sedia and Ehrenfeld, 2005), which is indicative of the limited nitrate availability for fungi associated with the bottom part of mosses and further supported the low expression level of fungal nitrate transporters in the bottom part of the mosses. Moreover, the "organonitrogen compound catabolic process" was detected as the most enriched GO term in the bottom layer of *D. scoparium* (Supporting Information Table S16). The overall increase of ammonium transporter activity in the bottom layer could be attributed to a high ammonium and low nitrate content beneath moss mats (Sedia and Ehrenfeld, 2005), high fungal activities in the lower layers (Davey *et al.*, 2013; Chen *et al.*, 2018), combined with a fungal preference for ammonium as an inorganic nitrogen source, and reduced competition with plants for the available ammonium at this location. *MEP*γ genes detected here represent one type of ammonium transporter genes, which have been reported across the fungal tree of life (McDonald *et al.*, 2012). The other type of ammonium transporter, *MEP*α, has only been found in lichen-forming fungi, so far. Despite occasional reports of lichen-forming fungi in the moss mycobiome (Davey *et al.*, 2013; Chen *et al.*, 2018), *MEP*α genes were not detected here, either because of low abundance of lichens in the community or because the *MEP*α genes are expressed at levels below the detection limit of this experiment.

Ammonium versus nitrate availability could also be linked to localized microbial communities. In our study, the nitrifying bacteria *Nitrosomonas* spp. were exclusively detected in the top two layers (Supporting Information Table S12) of *D. scoparium* and might provide nitrates to the healthy photosynthetic tissues of this moss and its associated fungal

community. Denitrification could also affect the relative ammonium and nitrate availability in this system. However, denitrifying bacteria are distributed across multiple phylogenetic groups and their denitrification capacity varies greatly even among closely related species (Jones *et al.*, 2008; Falcão Salles *et al.*, 2012), thus hindering valid measurement of their abundance in this study. Studies such as experiments involving nitrogen resources manipulation are needed to understand the nitrification activities in this focal system (Flores-Mireles *et al.*, 2007; Falcão Salles *et al.*, 2012). The two major nitrogen-fixing bacteria lineages, that is, *Cyanobacteria* and members of *Rhizobiales*, were both detected (Fig. 4). Members of the *Nostocales* (more specifically *Cylindrospermum* and *Nostoc*) were proportionately more abundant in the top layer than in the lower two layers (Fig. 4). Although the mechanisms for N transfer from these N-fixing bacteria to mosses (Warshan *et al.*, 2017) remain to be fully characterized, fungi might take advantage of the moss–bacteria association to obtain nitrogen. Fungi–bacteria–moss interactions appear to be complex and might involve other organisms, such as arthropod and algae that also inhabit mosses (Andrew *et al.*, 2003; Knapp and Lowe, 2009; Feng *et al.*, 2016). To disentangle these interactions, investigations combining microscopic observations, nutrient tracing and differential gene expression analyses in a simplified *in vitro* resynthesis system are needed.

Differential gene expression of fungal CAZy *along the senescence gradient of* Dicranum scoparium

Overall, *CAZy* genes were expressed more toward the bottom layer of *D. scoparium* gametophytes, which is in agreement with previous studies showing higher fungal nrRNA activity (Chen *et al.*, 2018) and fungal biomass (Davey *et al.*, 2012, 2013) in the bottom, decomposing, layer of moss gametophytes. Most fungi colonizing this bottom, partly decomposed, layer are expected to be saprophytic and use *CAZy* genes to actively contribute to the decomposition process. The nutrients released from the degradation of that bottom layer can be up taken by the local fungal community through various nutrient transporters. Of the top 30 expressed *CAZy* genes across the gametophytes, eight were classified as Auxiliary Activity family 2 (AA2), which contains class II lignin-modifying peroxidase (Cherry *et al.*, 1999). Mosses do not make wood or lignin. However, they are known to have lignin-like polymers (Roberts *et al.*, 2012). Multiple genes of Glycoside Hydrolases (GH7 and GH16) targeting the compounds of mosses' cell wall (pectin, cellulose and cross-linked glycan) (Roberts *et al.*, 2012) were detected among the most highly expressed *CAZy* genes throughout the moss (Fig. 3). Because mycorrhizal interactions with mosses have not been observed (Davey and Currah, 2006; Field *et al.*, 2015), it is unlikely that fungi associated with mosses transfer a fraction of these nutrients resulting from decomposition to the moss host using nutrient transporters. An alternative hypothesis is that some of the fungi that absorb nutrients released by the cellular breakdown of *D. scoparium* transfer part of these nutrients to nearby trees with which they form a mycorrhizal association (Carleton and Read, 1991). To test the latter hypothesis, isotope tracing of nutrient flow is required.

The taxonomic classification of fungal nutrient transporter and CAZy RNA revealed increase proportions of Basidiomycota toward the bottom layer of gametophytes, which is concordant with the results based on nrRNA data (Chen *et al.*, 2018). The healthy photosynthetic (top) portion of gametophytes are dominated by ascomycetes, especially members of Pezizomycotina (U'Ren *et al.*, 2010; Davey *et al.*, 2012, 2017; Chen *et al.*, 2018). This might suggest that basidiomycetes are better adapted to colonize senescent/decomposing tissues of plants, where they can successfully compete with ascomycetes as decomposers of the soil litter (Voříšková and Baldrian, 2013). However, Ascomycota contribute considerably to biological activities in the lower portions of *D. scoparium* gametophytes, suggesting that many Ascomycota fungi are adapted to both photosynthetic and senescing moss tissues, potentially with dual functions as biotrophs and saprotrophs. Based on nrRNA, Chen *et al.* (2018) reported several cases of what appears to be the same fungal species living in all three layers of *D. scoparium.* Whether this dual trophic capability can be activated within a single strain or not, will require well-designed *in vitro* moss–fungus resynthesis experiments. An alternative hypothesis would consist of certain degrees of community turnover along this senescence gradient (Davey *et al.*, 2017; Chen *et al.*, 2018) where endophytic fungi in the top layer are replaced by different, saprotrophic, strains in the bottom layer.

Differential gene expression of D. scoparium *across its senescence gradient*

Mosses being one of the early diverging embryophyte lineages, a better understanding of fungi–mosses interactions has important implications on their respective evolutions (Field *et al.*, 2015; Lutzoni *et al.*, 2018). Our previous study revealed that moss-associated fungal communities are structured according to the senescence gradient of *D. scoparium* (Chen *et al.*, 2018). Here we detected differential suites of genetic responses from the moss host (Fig. 5). Genes that are involved in plant hormone pathways of plant defense, such as jasmonic acid (JA), salicylic acid (SA), ethylene (ET) and abscisic acid (ABA), mostly had a higher expression in the top layer (Fig. 5). Genes for ROS (reactive oxidation species) production and structure reinforcement (e.g., callose synthase and deposition) were also more highly expressed in the top layer of the moss gametophytes (Fig. 5). Genes related to apoptosis of moss cells were detected in

both the top and bottom layers of gametophytes. Studies on the model moss *Physcomitrella patens* revealed that several defensive mechanisms are shared between mosses and other land plants (Bressendorff *et al.*, 2016; Ponce de León and Montesano, 2017), such as a functional *CERK1* gene and genes related to Systemic Acquired Resistance (SAR) and ROS. Another study demonstrated that *P. patens* releases peroxidases quickly to repel fungal invaders (Lehtonen *et al.*, 2009). Overall, this suggests that mosses utilize similar defensive mechanisms as other land plants.

Several plant genes related to nodulation formation were more expressed in the top layer of the moss and might be related to the *Rhizobiales* detected throughout the moss gametophytes (Fig. 4). *Rhizobiales* have been reported from various moss species and play important roles in peatland nitrogen fixation (Liu *et al.*, 2014; Leppänen *et al.*, 2015). The genetic mechanisms underlying moss–*Rhizobiales* interactions remain poorly known. Although we were able to extract reads belonging to the bacterial rRNA from our metatranscriptomic data, the transcripts of functional genes of prokaryotes were effectively removed during the poly-A enrichment mRNA library preparation step. Therefore, we are uncertain about the microbial source of the signal for plant genes involved with nodulation formation. Plant–arbuscular mycorrhizae share similar genetic components with plant–*Rhizobiales* symbioses (Delaux *et al.*, 2013). However, arbuscular mycorrhizal fungi were detected at very low levels in our samples (Chen *et al.*, 2018).

Experimental procedures

Environmental samples and metatranscriptome sequencing of Dicranum scoparium

Total RNA was extracted from three layers representing different senescence stages of *Dicranum scoparium* (Fig. 1, Supporting Information Fig. S1A; for more information see Chen *et al.*, 2018). For each layer, three replicates representing three microsites (10 m apart) were obtained for a total of nine samples for transcriptomic analyses. Each of the nine samples included approximately 20 moss stems. The sampling localities were in Duke Forest with mixed pine and deciduous trees (NC, USA, 36.010830°N, 78.967864°W). The sampling was conducted in the winter (January 2014) to maximize the detection of core community activities and minimize the chances of detecting random community assemblies that are likely to be present during hot and humid summers in Durham, North Carolina. Libraries for Illumina HiSeq sequencing were prepared using TruSeq mRNA stranded kits and were sequenced with the Illumina HiSeq 2000/2500 platform with 100 bp paired-end in one lane; for the sequencing quality, filtering and trimming criteria, see Chen *et al.* (2018). The raw reads of these nine samples are deposited in the Sequence Read Archive of NCBI GenBank (SRA accession number: PRJNA499105).

Metatranscriptome assembly and binning

Trimmomatic (Bolger *et al.*, 2014) was used to trim adaptors and to remove poor quality reads from the environmental samples of *D. scoparium.* SortMeRNA (Kopylova *et al.*, 2012) was used to remove eukaryotic and prokaryotic ribosomal RNAs. The remaining reads (mostly mRNA) were assembled with Trinity (Haas *et al.*, 2013) for each individual sample. The longest sequences of each component were pooled, clustered with 98% similarity using CD-HIT (Li and Godzik, 2006), and the longest sequences of each 98% contig were kept as representative sequences (Supporting Information Method S1). The representative sequences were searched against the UniProt database (accessed in 2014) (The UniProt, 2015) using the BLASTX (Camacho *et al.*, 2009) function, and only the top hits (E < 1e-6) were kept. The Organism Category information associated with the UniProt top hits was used to assign assembled transcripts into 11 categories (fungi, plants, human, invertebrates, vertebrates, *Archaea*, viruses, rodents, unclassified/no hits, *Bacteria*, mammals). The read mapping ratios were summarized with multiqc (Ewels *et al.*, 2016). Those transcripts with top hits as fungi were used for further analyses. All assembled transcripts are referred to as 'genes' in this article. Sequences of the assembled transcripts were deposited in the MG-RAST public server (accession: mgs699952) (Meyer, 2008).

Fungal Nutrient Transporters (amino acids [organic nitrogen], carbon, inorganic nitrogen, phosphorus and sulfur) Database (FNTD) and Fungal CAZy Database (FCD) construction

Assembled transcripts having top hits to fungi from the previous step were subjected to BLASTX using a customized data set of NCBI fungal nutrient-related sequences (for search keywords, see Supporting Information Method S2). Transcripts with *E* values < 1e-6 were kept. The *E*-value cutoff was selected based on previous studies (Hesse *et al.*, 2015; Quandt *et al.*, 2015; Comtet-Marre *et al.*, 2017; Meiser *et al.*, 2017; Gonzalez *et al.*, 2018) and after manual examination of a subset of sequences and their BLASTX results. To gain more taxonomic information and to confirm that the selected transcripts really belong to fungi, transcripts were first translated into proteins with Transdecoder (Haas *et al.*, 2013) and an additional round of BLASTP against the NCBI Non-Redundant (NR) protein database was performed, saving the top five hits. MEGAN (Huson *et al.*, 2007) was used to summarize the taxonomic affiliation of each transcript to

assure they belong to the fungal kingdom and to determine their phylum association (Supporting Information Fig. S1B). The Trinotate pipeline (Haas *et al.*, 2013), which integrates multiple annotation tools (BLASTX, BLASTP, UniProt, pfam) (Camacho *et al.*, 2009; The UniProt, 2015; Finn *et al.*, 2016), was used to generate annotation reports for transcripts belonging to fungi. All transcripts annotated as 'transporter' and 'transmembrane' were extracted and assigned to five nutrient categories (amino acids [organic nitrogen], carbon, inorganic nitrogen, phosphorus and sulfur) when applicable (for key words, see Supporting Information Methods S2). When these annotations included Major Facilitator Superfamily (MFS) genes, the sequences were annotated manually to determine whether they were associated with any of our five selected nutrient types. If not, the sequences were discarded from the FNTD database (Supporting Information Fig. S1B). The **F**ungal **C**AZy **D**atabase (FCD) workflow was similar to the FNTD workflow, except for the BLASTX search that was from dbCAN (http://csbl.bmb.uga.edu/dbCAN/download.php) (Supporting Information Fig. S1C).

Axenic Dicranum scoparium *Transcriptome Database (ADTD) construction*

Axenic cultures of *Dicranum scoparium* were prepared from spores in enclosed capsules (collected at Telico Plains, TN, on July 7, 2009, ID: HBK013) that were surface sterilized with 10% sodium hypochlorite for 30 s (Vujičić *et al.*, 2009). The moss was grown using Murashige and Skoog media (Murashige and Skoog, 1962) with 1.5% sucrose (Vujičić *et al.*, 2009) in Magna jars (Supporting Information Fig. 1D) for 3.5 months prior to RNA extraction. To confirm that the *D. scoparium* axenic culture prepared from a Tennessee population is closely related to the field collected *D. scoparium* from Duke Forest, North Carolina, sequences of two plant barcoding genes, the large subunit of the ribulose-bisphosphate carboxylase gene (*rbcL*) and the Internal Transcribed Spacer (ITS) region of ribosomal RNA (Qiu *et al.*, 2006; Lang and Stech, 2014) were extracted from our transcriptomic data. The *rbcL* and ITS sequences from the two *D. scoparium* populations (accession number *rbcL*: MK463856 [Duke Forest], MK463855 [Tennessee]; ITS: MK457127 [Duke Forest], MK457126 [Tennessee]) were confirmed to be identical, validating the use of axenic culture transcriptome generated from the Tennessee population as reference for the analysis. To confirm that the moss culture was free of fungi, PCR with a universal fungal rRNA primer pair ITS1F and LR3 (U'Ren, 2011) was performed, followed by gel electrophoresis examination. RNAseq library preparation was done with the Illumina mRNA-stranded RNAseq kit. Sequencing was performed with Illumina HiSeq4000 (150 bp paired-end) at the Duke Genomic and Computational Biology facility. Quality filtering and assembly were the same as described above. The annotation was performed using the Trinotate pipeline (Haas *et al.*, 2013). For scripts and details of workflow, see Supporting Information Method S1 and Fig. S1D. For quality and rRNA removal report, see Supporting Information Table S1. The annotations of differentially expressed genes were searched for key words related to plant defense/symbiosis (for key words, see Supporting Information Methods S3).

DGE test

RNAseq reads from the sampled *D. scoparium* gametophytes were mapped to FNTD, FCD and ADTD separately (Supporting Information Fig. S1) with Bowtie2 (Langmead and Salzberg, 2012). The read mapping reports were generated with Idxtat in Samtool (Li *et al.*, 2009). The Wald test was implemented using the DEseq2 package (Love *et al.*, 2014). Gene Ontology (GO) enrichment analyses for differentially expressed gene sets were performed in GoSeq (Young *et al.*, 2010).

Phylogenetic analyses of ammonium transporters

We conducted phylogenetic analyses to determine the relationships of the fungal ammonium transporters detected here to the known ammonium transporter/methylammonium permease/Rhesus factor (AMT/MEP/Rh) gene family. We aligned sequences detected in this study with a published alignment containing 513 reference sequences from different kingdoms (McDonald *et al.*, 2012). Nine fungal ammonium transporters were downloaded from NCBI and added to the alignment (Supporting Information Table S2). All sequences were first aligned with MAFFT (Katoh and Standley, 2013) and then manually checked using Aliview (Larsson, 2014). A total of 1020 characters and 662 sequences were included. Phylogenies were inferred with maximum likelihood as an optimality criterion using RAxML-HPC2 v8.2.10 (Stamatakis, 2014) available on the CIPRES portal (Miller *et al.*, 2010). The substitution model and partition scheme were determined using the program PartitionFinder (Lanfear *et al.*, 2012) prior to phylogeny reconstruction. The GTRGAMMA substitution model was selected, and partitions were set for each codon position. Rapid bootstrap search of 1000 replicates was conducted. For graph preparation, Figtree (http://tree.bio.ed.ac.uk/software/figtree/) and ggtree (Yu *et al.*, 2017) were used.

Assessment of active bacterial communities of Dicranum scoparium

Short reads of the environmental *D. scoparium* metatranscriptomes were mapped against the SILVA 16s rRNA

reference (accessed on Nov. 2014) (Quast *et al.*, 2013) using Bowtie2 (Langmead and Salzberg, 2012). The forward and reverse 16S reads belonging to bacteria were then merged with USEARCH (Edgar, 2013). The merged reads were megaBLASTed against NCBI GenBank, and the results were summarized with MEGAN using the lowest common ancestor assigning algorithm (Huson *et al.*, 2007). All reads mapped to the chloroplast and mitochondria genomes were discarded.

Conclusion

Fungal nutrient-related transporters and CAZys examined here were most highly expressed in the bottom layer of the gametophytes. For nitrogen-related fungal transporters, this trend was driven by ammonium transporters, which we further identified phylogenetically as *MEP*γ genes. Fungal nitrate transporters, however, were more highly expressed in the top layer, suggesting differential inorganic nitrogen (Fellbaum *et al.*, 2012) utilizations for fungi in the top layer versus the bottom layer. We found that Basidiomycota are metabolically more active toward the bottom layers, mainly as decomposers, which is in agreement with our previous observation based on nrRNA data (Chen *et al.*, 2018). Ascomycota are metabolically more active than Basidiomycota in the top photosynthetic layer, which is consistent with diversity studies on fungal endophytes, demonstrating that the great majority of fungal endophytes are classified within the subphylum Pezizomycotina (Rodriguez *et al.*, 2009). Bacterial communities were also revealed by rRNA data in the metatranscriptomes. The nitrogen fixers – *Cyanobacteria* and *Rhizobiales* – were both detected. *Cyanobacteria* are more abundant in the top layer while *Rhizobiales* were more or less evenly distributed across the senescence gradient. We detected an array of moss genes significantly differentially expressed in the top versus bottom of the moss that are likely to be involved in microbe recognition and defense/symbiosis interactions similar to other land plants. In addition, one of the most enriched plant GO term in the bottom layer of this moss is “organonitrogen compound catabolic process”, which echoes the high activities of fungal ammonium transporters in the bottom portion of *D. scoparium.* This moss represents an ideal system to study the longstanding hypothesis that many endophytic fungi have the capacity to switch between endophytism and saprotrophism. This functional transition was revealed here by an array of differentially expressed fungal genes based on metatranscriptomic data. The gene sequences and taxa detected by this study provide a strong foundation at the community level to understand whether functional transitions of fungal activities between endophytism and saprotrophism could occur within one strain or even one mycelium. Experiments using an *in vitro* plant–fungal coculture system are needed to address the new hypotheses emerging from this study.

Acknowledgements

We thank Hailee Korotkin and Brandon Matheny for sharing the axenic culture of *Dicranum scoparium*; Alejo Rojas, Jolanta Miadlikowska and Steven Wu for providing comments on this manuscript; and Daniele Armaleo for discussions throughout this project. We are thankful to the Duke Compute Cluster for providing computational resources. This project was funded by the National Science Foundation (NSF) grants DEB-1046065 and DEB-1541548 to FL, and the NSF Doctoral Dissertation Improvement Grant (DEB-1701836) to K-HC and FL. We are grateful for the generous research awards from the Mycological Society of America and for support from Duke University to K-HC. We also thank the anonymous reviewers for their comments.

References

Almario, J., Jeena, G., Wunder, J., Langen, G., Zuccaro, A., Coupland, G., and Bucher, M. (2017) Root-associated fungal microbiota of nonmycorrhizal *Arabis alpina* and its contribution to plant phosphorus nutrition. *Proc Natl Acad Sci* **114**: E9403–E9412.

Andrew, N.R., Rodgerson, L., and Dunlop, M. (2003) Variation in invertebrate–bryophyte community structure at different spatial scales along altitudinal gradients. *J Biogeogr* **30**: 731–746.

Barnes, C.J., van der Gast, C.J., McNamara, N.P., Rowe, R., and Bending, G.D. (2018) Extreme rainfall affects assembly of the root-associated fungal community. *New Phytol* **220**: 1172–1184.

Bolger, A.M., Lohse, M., and Usadel, B. (2014) Trimmomatic: a flexible trimmer for Illumina sequence data. *Bioinformatics* **30**: 2114–2120.

Bonfante, P., and Genre, A. (2010) Mechanisms underlying beneficial plant-fungus interactions in mycorrhizal symbiosis. *Nat Commun* **1**: 48.

Bonito, G., Reynolds, H., Robeson, M.S., Nelson, J., Hodkinson, B.P., Tuskan, G., *et al.* (2014) Plant host and soil origin influence fungal and bacterial assemblages in the roots of woody plants. *Mol Ecol* **23**: 3356–3370.

Bressendorff, S., Azevedo, R., Kenchappa, C.S., Ponce de León, I., Olsen, J.V., Rasmussen, M.W., *et al.* (2016) An innate immunity pathway in the Moss *Physcomitrella patens*. *Plant Cell* **28**: 1328–1342.

Brown, D.H., and Bates, J.W. (1990) Bryophytes and nutrient cycling. *Bot J Linn Soc* **104**: 129–147.

Camacho, C., Coulouris, G., Avagyan, V., Ma, N., Papadopoulos, J., Bealer, K., and Madden, T. (2009) BLAST+: architecture and applications. *BMC Bioinformatics* **10**: 421.

Carleton, T.J., and Read, D.J. (1991) Ectomycorrhizas and nutrient transfer in conifer-feather moss ecosystems. *Can J Bot* **69**: 778–785.

Ceccaroli, P., Buffalini, M., Saltarelli, R., Barbieri, E., Polidori, E., Ottonello, S., *et al.* (2010) Genomic profiling

of carbohydrate metabolism in the ectomycorrhizal fungus tuber melanosporum. *New Phytol* **189**: 751–764.

Chang, H.-X., Yendrek, C.R., Caetano-Anolles, G., and Hartman, G.L. (2016) Genomic characterization of plant cell wall degrading enzymes and in silico analysis of xylanses and polygalacturonases of *Fusarium virguliforme*. *BMC Microbiol* **16**: 147.

Chen, K.-H., Liao, H.-L., Arnold, A.E., Bonito, G., and Lutzoni, F. (2018) RNA-based analyses reveal fungal communities structured by a senescence gradient in the moss *Dicranum scoparium* and the presence of putative multi-trophic fungi. *New Phytol* **218**: 1596–1611.

Chen, Y.-L., Kauffman, S., and Reynolds, T.B. (2008) *Candida albicans* uses multiple mechanisms to acquire the essential metabolite inositol during infection. *Infect Immun* **76**: 2793–2801.

Cherry, J.R., Lamsa, M.H., Schneider, P., Vind, J., Svendsen, A., Jones, A., and Pedersen, A.H. (1999) Directed evolution of a fungal peroxidase. *Nat Biotechnol* **17**: 379–384.

Comtet-Marre, S., Parisot, N., Lepercq, P., Chaucheyras-Durand, F., Mosoni, P., Peyretaillade, E., *et al.* (2017) Metatranscriptomics reveals the active bacterial and eukaryotic fibrolytic communities in the rumen of dairy cow fed a mixed diet. *Front Microbiol* **8**: 67.

Davey, M.L., and Currah, R.S. (2007) A new species of *Cladophialophora* (hyphomycetes) from boreal and montane bryophytes. *Mycol Res* **111**: 106–116.

Davey, M.L., and Currah, R.S. (2006) Interactions between mosses (Bryophyta) and fungi. *Can J Bot* **84**: 1509–1519.

Davey, M.L., Heegaard, E., Halvorsen, R., Kauserud, H., and Ohlson, M. (2013) Amplicon-pyrosequencing-based detection of compositional shifts in bryophyte-associated fungal communities along an elevation gradient. *Mol Ecol* **22**: 368–383.

Davey, M.L., Heegaard, E., Halvorsen, R., Ohlson, M., and Kauserud, H. (2012) Seasonal trends in the biomass and structure of bryophyte-associated fungal communities explored by 454 pyrosequencing. *New Phytol* **195**: 844–856.

Davey, M.L., Skogen, M.J., Heegaard, E., Halvorsen, R., Kauserud, H., and Ohlson, M. (2017) Host and tissue variations overshadow the response of boreal moss-associated fungal communities to increased nitrogen load. *Mol Ecol* **26**: 571–588.

Delaux, P.-M., Séjalon-Delmas, N., Bécard, G., and Ané, J.-M. (2013) Evolution of the plant-microbe symbiotic toolkit. *Trends Plant Sci* **18**: 298–304.

Eastwood, D.C., Floudas, D., Binder, M., Majcherczyk, A., Schneider, P., Aerts, A., *et al.* (2011) The plant cell wall-decomposing machinery underlies the functional diversity of forest fungi. *Science* **333**: 762–765.

Edgar, R.C. (2013) UPARSE: highly accurate OTU sequences from microbial amplicon reads. *Nat Methods* **10**: 996–998.

Ewels, P., Magnusson, M., Lundin, S., and Käller, M. (2016) MultiQC: summarize analysis results for multiple tools and samples in a single report. *Bioinformatics* **32**: 3047–3048.

Falcão Salles, J., Le Roux, X., and Poly, F. (2012) Relating phylogenetic and functional diversity among denitrifiers and quantifying their capacity to predict community functioning. *Front Microbiol* **3**: 209.

Fellbaum, C.R., Gachomo, E.W., Beesetty, Y., Choudhari, S., Strahan, G.D., Pfeffer, P.E., *et al.* (2012) Carbon availability triggers fungal nitrogen uptake and transport in arbuscular mycorrhizal symbiosis. *Proc Natl Acad Sci U S A* **109**: 2666–2671.

Feng, J., Guo, Y., Zhang, X., Wang, G., Lv, J., Liu, Q., and Xie, S. (2016) Identification and characterization of a symbiotic alga from soil bryophyte for lipid profiles. *Biol Open* **5**: 1317–1323.

Field, K.J., Pressel, S., Duckett, J.G., Rimington, W.R., and Bidartondo, M.I. (2015) Symbiotic options for the conquest of land. *Trends Ecol Evol* **30**: 477–486.

Finlay, R.D., Frostegård, Å., and Sonnerfeldt, A.-M. (1992) Utilization of organic and inorganic nitrogen sources by ectomycorrhizal fungi in pure culture and in symbiosis with *Pinus contorta* Dougl. ex Loud. *New Phytol* **120**: 105–115.

Finn, R.D., Coggill, P., Eberhardt, R.Y., Eddy, S.R., Mistry, J., Mitchell, A.L., *et al.* (2016) The Pfam protein families database: towards a more sustainable future. *Nucleic Acids Res* **44**: D279–D285.

Flores-Mireles, A.L., Winans, S.C., and Holguin, G. (2007) Molecular characterization of diazotrophic and denitrifying bacteria associated with mangrove roots. *Appl Environ Microbiol* **73**: 7308–7321.

Gahan, J., and Schmalenberger, A. (2014) The role of bacteria and mycorrhiza in plant sulfur supply. *Front Plant Sci* **5**: 723.

Giovanelli, J. (1987) Sulfur amino acids of plants: an overview. In *Methods in Enzymology*: Academic Press, pp. 419–426.

Glassman, S.I., Wang, I.J., and Bruns, T.D. (2017) Environmental filtering by pH and soil nutrients drives community assembly in fungi at fine spatial scales. *Mol Ecol* **26**: 6960–6973.

Gonzalez, E., Pitre, F.E., Pagé, A.P., Marleau, J., Guidi Nissim, W., St-Arnaud, M., *et al.* (2018) Trees, fungi and bacteria: tripartite metatranscriptomics of a root microbiome responding to soil contamination. *Microbiome* **6**: 53.

Haas, B.J., Papanicolaou, A., Yassour, M., Grabherr, M., Blood, P.D., Bowden, J., *et al.* (2013) *De novo* transcript sequence reconstruction from RNA-seq using the Trinity platform for reference generation and analysis. *Nat Protoc* **8**: 1494–1512.

Hall, J.L., and Williams, L.E. (2000) Assimilate transport and partitioning in fungal biotrophic interactions. *Funct Plant Biol* **27**: 549–560.

van der Heijden, M.G.A., Martin, F.M., Selosse, M.-A., and Sanders, I.R. (2015) Mycorrhizal ecology and evolution: the past, the present, and the future. *New Phytol* **205**: 1406–1423.

Hesse, C.N., Mueller, R.C., Vuyisich, M., Gallegos-Graves, L.V., Gleasner, C.D., Zak, D.R., and Kuske, C.R. (2015) Forest floor community metatranscriptomes identify fungal and bacterial responses to N deposition in two maple forests. *Front Microbiol* **6**: 337.

Huson, D.H., Auch, A.F., Qi, J., and Schuster, S.C. (2007) MEGAN analysis of metagenomic data. *Genome Res* **17**: 377–386.

Jones, C.M., Stres, B., Rosenquist, M., and Hallin, S. (2008) Phylogenetic analysis of nitrite, nitric oxide, and nitrous oxide respiratory enzymes reveal a complex evolutionary history for denitrification. *Mol Biol Evol* **25**: 1955–1966.

Katoh, K., and Standley, D.M. (2013) MAFFT multiple sequence alignment software version 7: improvements in performance and usability. *Mol Biol Evol* **30**: 772–780.

Keller, G. (1996) Utilization of inorganic and organic nitrogen sources by high-subalpine ectomycorrhizal fungi of *Pinus cembra* in pure culture. *Mycol Res* **100**: 989–998.

Knapp, J.M., and Lowe, R.L. (2009) Spatial distribution of epiphytic diatoms on lotic bryophytes. *Southeast Nat* **8**: 305–316.

Kohler, A., Kuo, A., Nagy, L.G., Morin, E., Barry, K.W., Buscot, F., *et al.* (2015) Convergent losses of decay mechanisms and rapid turnover of symbiosis genes in mycorrhizal mutualists. *Nat Genet* **47**: 410–415.

Kopylova, E., Noé, L., and Touzet, H. (2012) SortMeRNA: fast and accurate filtering of ribosomal RNAs in metatranscriptomic data. *Bioinformatics* **28**: 3211–3217.

Lanfear, R., Calcott, B., Ho, S.Y.W., and Guindon, S. (2012) PartitionFinder: combined selection of partitioning schemes and substitution models for phylogenetic analyses. *Mol Biol Evol* **29**: 1695–1701.

Lang, A., and Stech, M. (2014) What's in a name? Disentangling the *Dicranum scoparium* species complex (Dicranaceae, Bryophyta). *Syst Bot* **39**: 369–379.

Langmead, B., and Salzberg, S.L. (2012) Fast gapped-read alignment with Bowtie 2. *Nat Meth* **9**: 357–359.

Larsson, A. (2014) AliView: a fast and lightweight alignment viewer and editor for large datasets. *Bioinformatics* **30**: 3276–3278.

Lehtonen, M.T., Akita, M., Kalkkinen, N., Ahola-Iivarinen, E., Rönnholm, G., Somervuo, P., *et al.* (2009) Quickly-released peroxidase of moss in defense against fungal invaders. *New Phytol* **183**: 432–443.

Lenton, T.M., Dahl, T.W., Daines, S.J., Mills, B.J.W., Ozaki, K., Saltzman, M.R., and Porada, P. (2016) Earliest land plants created modern levels of atmospheric oxygen. *Proc Natl Acad Sci U S A* **113**: 9704–9709.

Leppänen, S.M., Rissanen, A.J., and Tiirola, M. (2015) Nitrogen fixation in *Sphagnum* mosses is affected by moss species and water table level. *Plant and Soil* **389**: 185–196.

Li, H., Handsaker, B., Wysoker, A., Fennell, T., Ruan, J., Homer, N., *et al.* (2009) The sequence alignment/map format and SAMtools. *Bioinformatics* **25**: 2078–2079.

Li, W., and Godzik, A. (2006) CD-HIT: a fast program for clustering and comparing large sets of protein or nucleotide sequences. *Bioinformatics* **22**: 1658–1659.

Liao, H.-L., Chen, Y., and Vilgalys, R. (2016) Metatranscriptomic study of common and host-specific patterns of gene expression between pines and their symbiotic ectomycorrhizal fungi in the genus *Suillus*. *PLoS Genet* **12**: e1006348.

Linder, T. (2012) Genomics of alternative sulfur utilization in ascomycetous yeasts. *Microbiology* **158**: 2585–2597.

Liu, B., Lei, C., Jin, J., Guan, Y., Li, S., Zhang, Y., and Liu, W. (2016) Physiological responses of two moss species to the combined stress of water deficit and elevated N deposition (II): carbon and nitrogen metabolism. *Ecol Evol* **6**: 7596–7609.

Liu, X.L., Liu, S.L., Liu, M., Kong, B.H., Liu, L., and Li, Y.H. (2014) A primary assessment of the endophytic bacterial community in a xerophilous moss (*Grimmia montana*) using molecular method and cultivated isolates. *Braz J Microbiol* **45**: 165–173.

Liu, X.-Y., Koba, K., Makabe, A., Li, X.-D., Yoh, M., and Liu, C.-Q. (2013) Ammonium first: natural mosses prefer atmospheric ammonium but vary utilization of dissolved organic nitrogen depending on habitat and nitrogen deposition. *New Phytol* **199**: 407–419.

Lo Presti, L., Lanver, D., Schweizer, G., Tanaka, S., Liang, L., Tollot, M., *et al.* (2015) Fungal effectors and plant susceptibility. *Annu Rev Plant Biol* **66**: 513–545.

Love, M., Huber, W., and Anders, S. (2014) Moderated estimation of fold change and dispersion for RNA-seq data with DESeq2. *Genome Biol* **15**: 550.

Lutzoni, F., Nowak, M.D., Alfaro, M.E., Reeb, V., Miadlikowska, J., Krug, M., *et al.* (2018) Contemporaneous radiations of fungi and plants linked to symbiosis. *Nat Commun* **9**: 5451.

Martin, F., Kohler, A., Murat, C., Balestrini, R., Coutinho, P. M., Jaillon, O., *et al.* (2010) Périgord black truffle genome uncovers evolutionary origins and mechanisms of symbiosis. *Nature* **464**: 1033–1038.

Martino, E., Morin, E., Grelet, G.-A., Kuo, A., Kohler, A., Daghino, S., *et al.* (2018) Comparative genomics and transcriptomics depict ericoid mycorrhizal fungi as versatile saprotrophs and plant mutualists. *New Phytol* **217**: 1213–1229.

McDonald, T.R., Dietrich, F.S., and Lutzoni, F. (2012) Multiple horizontal gene transfers of ammonium transporters/ammonia permeases from prokaryotes to eukaryotes: toward a new functional and evolutionary classification. *Mol Biol Evol* **29**: 51–60.

Meiser, A., Otte, J., Schmitt, I., and Grande, F.D. (2017) Sequencing genomes from mixed DNA samples—evaluating the metagenome skimming approach in lichenized fungi. *Sci Rep* **7**: 14881.

Meyer, F. (2008) The metagenomics RAST server—a public resource for the automatic phylogenetic and functional analysis of metagenomes. *BMC Bioinformatics* **9**: 1471-2105.

Miller, M.A., Pfeiffer, W., and Schwartz, T. (2010) Creating the CIPRES Science Gateway for inference of large phylogenetic trees.

Murashige, T., and Skoog, F. (1962) A revised medium for rapid growth and bioassays with tobacco tissue cultures. *Physiol Plant* **15**: 473–497.

O'Connell, R.J., Thon, M.R., Hacquard, S., Amyotte, S.G., Kleemann, J., Torres, M.F., *et al.* (2012) Lifestyle transitions in plant pathogenic *Colletotrichum* fungi deciphered by genome and transcriptome analyses. *Nat Genet* **44**: 1060–1065.

Ohm, R.A., Feau, N., Henrissat, B., Schoch, C.L., Horwitz, B.A., Barry, K.W., *et al.* (2012) Diverse lifestyles and strategies of plant pathogenesis encoded in the genomes of eighteen Dothideomycetes Fungi. *PLoS Pathog* **8**: e1003037.

Osono, T., and Hirose, D. (2011) Colonization and lignin decomposition of pine needle litter by *Lophodermium pinastri*. *For Pathol* **41**: 156–162.

Peay, K.G., Kennedy, P.G., and Talbot, J.M. (2016) Dimensions of biodiversity in the Earth mycobiome. *Nat Rev Microbiol* **14**: 434–447.

Plett, J.M., Daguerre, Y., Wittulsky, S., Vayssières, A., Deveau, A., Melton, S.J., *et al.* (2014) Effector MiSSP7 of the mutualistic fungus *Laccaria bicolor* stabilizes the *Populus* JAZ6 protein and represses jasmonic acid (JA) responsive genes. *Proc Natl Acad Sci U S A* **111**: 8299–8304.

Ponce de León, I., and Montesano, M. (2017) Adaptation mechanisms in the evolution of moss defenses to microbes. *Front Plant Sci* **8**: 366.

Puttick, M.N., Morris, J.L., Williams, T.A., Cox, C.J., Edwards, D., Kenrick, P., *et al.* (2018) The interrelationships of land plants and the nature of the ancestral Embryophyte. *Curr Biol* **28**: 733–745.e2.

Qiu, Y.-L., Li, L., Wang, B., Chen, Z., Knoop, V., Groth-Malonek, M., *et al.* (2006) The deepest divergences in land plants inferred from phylogenomic evidence. *Proc Natl Acad Sci* **103**: 15511–15516.

Quandt, C.A., Kohler, A., Hesse, C.N., Sharpton, T.J., Martin, F., and Spatafora, J.W. (2015) Metagenome sequence of *Elaphomyces granulatus* from sporocarp tissue reveals Ascomycota ectomycorrhizal fingerprints of genome expansion and a Proteobacteria-rich microbiome. *Environ Microbiol* **17**: 2952–2968.

Quast, C., Pruesse, E., Yilmaz, P., Gerken, J., Schweer, T., Yarza, P., *et al.* (2013) The SILVA ribosomal RNA gene database project: improved data processing and web-based tools. *Nucleic Acids Res* **41**: D590–D596.

Riley, R., Salamov, A.A., Brown, D.W., Nagy, L.G., Floudas, D., Held, B.W., *et al.* (2014) Extensive sampling of basidiomycete genomes demonstrates inadequacy of the white-rot/brown-rot paradigm for wood decay fungi. *Proc Natl Acad Sci U S A* **111**: 9923–9928.

Roberts, A., Roberts, E., and Haigler, C. (2012) Moss cell walls: structure and biosynthesis. *Front Plant Sci* **3**: 166.

Rodriguez, R.J., White Jr, J.F., Arnold, A.E., and Redman, R.S. (2009) Fungal endophytes: diversity and functional roles. *New Phytol* **182**: 314–330.

Rudgers, J.A., Kivlin, S.N., Whitney, K.D., Price, M.V., Waser, N.M., and Harte, J. (2014) Responses of high-altitude graminoids and soil fungi to 20 years of experimental warming. *Ecology* **95**: 1918–1928.

Sedia, E.G., and Ehrenfeld, J.G. (2005) Differential effects of lichens, mosses and grasses on respiration and nitrogen mineralization in soils of the New Jersey Pinelands. *Oecologia* **144**: 137–147.

Sparks, J.P., Walker, J., Turnipseed, A., and Guenther, A. (2007) Dry nitrogen deposition estimates over a forest experiencing free air CO_2 enrichment. *Glob Change Biol* **14**: 768–781.

Stamatakis, A. (2014) RAxML Version 8: a tool for phylogenetic analysis and post-analysis of large phylogenies. *Bioinformatics* **30**: 1312–1313.

Stenroos, S., Laukka, T., Huhtinen, S., Döbbeler, P., Myllys, L., Syrjänen, K., and Hyvönen, J. (2010) Multiple origins of symbioses between ascomycetes and bryophytes suggested by a five-gene phylogeny. *Cladistics* **26**: 281–300.

Struck, C. (2015) Amino acid uptake in rust fungi. *Front Plant Sci* **6**: 40.

Talbot, J.M., Bruns, T.D., Taylor, J.W., Smith, D.P., Branco, S., Glassman, S.I., *et al.* (2014) Endemism and functional convergence across the north American soil mycobiome. *Proc Natl Acad Sci U S A* **111**: 6341–6346.

The UniProt, C. (2015) UniProt: a hub for protein information. *Nucleic Acids Res* **43**: D204–D212.

Turetsky, M.R. (2003) The role of Bryophytes in carbon and nitrogen cycling. *The Bryologist* **106**: 395–409.

U'Ren, J.M. (2011) Host-, geographic-, and ecological specificity of endophytic and endolichenic fungal communities. PhD Thesis. Tucson, AZ, USA: University of Arizona.

U'Ren, J.M., Lutzoni, F., Miadlikowska, J., and Arnold, A.E. (2010) Community analysis reveals close affinities between endophytic and endolichenic fungi in mosses and lichens. *Microb Ecol* **60**: 340–353.

U'Ren, J.M., Lutzoni, F., Miadlikowska, J., Laetsch, A.D., and Arnold, A.E. (2012) Host and geographic structure of endophytic and endolichenic fungi at a continental scale. *Am J Bot* **99**: 898–914.

Verslues, P.E., and Sharma, S. (2010) Proline metabolism and its implications for plant-environment interaction. *Arab Book Am Soc Plant Biol* **8**: e0140.

Voříšková, J., and Baldrian, P. (2013) Fungal community on decomposing leaf litter undergoes rapid successional changes. *ISME J* **7**: 477–486.

Vujičić, M., Sabovljević, A., and Sabovljević, M. (2009) Axenically culturing the bryophytes: a case study of the moss *Dicranum scoparium* Hedw. Dicranaceae, Bryophyta. *Bot Serbica* **33**: 137–140.

Walker, J.K.M., Cohen, H., Higgins, L.M., and Kennedy, P. G. (2014) Testing the link between community structure and function for ectomycorrhizal fungi involved in a global tripartite symbiosis. *New Phytol* **202**: 287–296.

Wang, X., Zhang, X., Liu, L., Xiang, M., Wang, W., Sun, X., *et al.* (2015) Genomic and transcriptomic analysis of the endophytic fungus *Pestalotiopsis fici* reveals its lifestyle and high potential for synthesis of natural products. *BMC Genomics* **16**: 28.

Warshan, D., Espinoza, J.L., Stuart, R.K., Richter, R.A., Kim, S.-Y., Shapiro, N., *et al.* (2017) Feathermoss and epiphytic *Nostoc* cooperate differently: expanding the spectrum of plant-cyanobacteria symbiosis. *ISME J* **11**: 2821–2833.

Xie, X., Lin, H., Peng, X., Xu, C., Sun, Z., Jiang, K., *et al.* (2016) Arbuscular mycorrhizal symbiosis requires a phosphate transceptor in the *Gigaspora margarita* fungal symbiont. *Mol Plant* **9**: 1583–1608.

Xue, C. (2012) Cryptococcus and beyond—inositol utilization and its implications for the emergence of fungal virulence. *PLoS Pathog* **8**: e1002869.

Yang, J., Yan, R., Roy, A., Xu, D., Poisson, J., and Zhang, Y. (2015) The I-TASSER Suite: protein structure and function prediction. *Nat Meth* **12**: 7–8.

Young, M.D., Wakefield, M.J., Smyth, G.K., and Oshlack, A. (2010) Gene ontology analysis for RNA-seq: accounting for selection bias. *Genome Biol* **11**: R14.

Yu, G., Smith, D.K., Zhu, H., Guan, Y., and Lam, T.T.-Y. (2017) Ggtree: an r package for visualization and annotation of phylogenetic trees with their covariates and other associated data. *Methods Ecol Evol* **8**: 28–36.

Zhao, Z., Liu, H., Wang, C., and Xu, J.-R. (2013) Comparative analysis of fungal genomes reveals different plant cell wall degrading capacity in fungi. *BMC Genomics* **14**: 274.

Zhou, J., Li, X., Huang, P.-W., and Dai, C.-C. (2018) Endophytism or saprophytism: decoding the lifestyle transition of the generalist fungus *Phomopsis liquidambari*. *Microbiol Res* **206**: 99–112.

Zhou, Z., Takaya, N., Nakamura, A., Yamaguchi, M., Takeo, K., and Shoun, H. (2002) Ammonia fermentation, a novel anoxic metabolism of nitrate by fungi. *J Biol Chem* **277**: 1892–1896.

Zuccaro, A., Lahrmann, U., Güldener, U., Langen, G., Pfiffi, S., Biedenkopf, D., *et al.* (2011) Endophytic life strategies decoded by genome and transcriptome analyses of the mutualistic root symbiont *Piriformospora indica*. *PLoS Pathog* **7**: e1002290.

Supporting Information

Additional Supporting Information may be found in the online version of this article at the publisher's web-site:

Table S1. Axenic *Dicranum scoparium* transcriptome reads quality report and assembly.

Table S2. Additional fungal ammonium transporter/methylammonium permease/Rhesus factor family reference sequences included for phylogenetic analyses.

Table S3. Fungal amino acid (organic nitrogen) transporters recovered from *D. scoparium* metatranscriptome.

Table S4. Fungal carbon transporters recovered from *D. scoparium* metatranscriptome.

Table S5. Fungal inorganic nitrogen transporters recovered from *D. scoparium* metatranscriptome.

Table S6. Fungal phosphorus transporters recovered from *D. scoparium* metatranscriptome.

Table S7. Fungal sulfur transporters recovered from *D. scoparium* metatranscriptome.

Table S8. The ratios of nutrient-type assignment for fungal nutrient transporter.

Table S9. The ratios of phylum assignment for fungal nutrient transporter.

Table S10. Fungal CAZy family and phylum/subphylum assignment of transcripts.

Table S11. The ratios of phyla assignment for CAZy genes.

Table S12. Ratio of reads mapped to bacteria classified at the genus level (defined as the lowest common ancestor by MEGAN). Yellow background highlights bacteria belonging to *Cyanobacteria* and *Rhizobiales.* Red background highlights *Nitrosomonas.*

Table S13. Significantly differentially expressed *D. scoparium* genes in the top layer versus the bottom layer (FDR < 0.01).

Table S14. Significantly differentially expressed *D. scoparium* genes in the bottom layer versus the top layer (FDR < 0.01).

Table S15. GO terms for highly expressed genes of *D. scoparium* in the top layer (P < 0.05).

Table S16. GO terms for highly expressed genes of *D. scoparium* in the bottom layer (P < 0.05).

Fig. S1. (a) Schematic workflow for environmental *Dicranum scoparium* sampling and subsequent read mapping; (b) workflow for Fungal Nutrient Transporter Database (FNTD) construction; (c) workflow for assembling the Fungal CAZy Database (FCD); (d) workflow for Axenic *Dicranum scoparium* Transcriptome Database (ADTD) construction.

Fig. S2. Percentage of reads mapped to assembled transcripts assigned to 10 taxonomic groups.

Fig. S3. Principal coordinate analyses of (a) Fungal Nutrient Transporters (FNTD), (b) fungal CAZy *(*FCD) and (c) axenic *Dicranum scoparium* (ADTD) expression levels across replicates and senescence layers of *D. scoparium*.

Fig. S4. Taxonomic distribution of 3112 fungal nutrient transporter genes (amino acids [organic nitrogen], carbon, inorganic nitrogen, phosphorus and sulfur) found in fungal communities associated with *Dicranum scoparium*.

Fig. S5. Ammonium transporter/methylammonium permease/Rhesus factor (AMT/MEP/Rh) gene family ML tree. Nomenclature of the gene clades follows Mcdonald *et al.* (2012). Red asterisks show phylogenetic placement of ammonium transporters we detected from fungi associated with *Dicranum scoparium*.

Fig. S6. Expression levels of commonly expressed LRR/defense/symbiosis-related genes of *D. scoparium* in the top and bottom layers.

Fig. S7. Differentially expressed genes of *D. scoparium* associated with enriched catabolic processes (GO term enriched, P < 0.05).

Supplementary Method S1: Scripts used in this study.

Supplementary Method S2: Keywords for retrieving fungal nutrient-related sequences from GenBank.

Supplementary Method S3: Key words used to extract plant defense and symbiosis genes from annotated transcriptomes.